TECHNICAL UNIVERSITY OF CLUJ-NAPOCA

ACTA TECHNICA NAPOCENSIS

Series: Applied Mathematics, Mechanics, and Engineering
Vol. 69, Issue II, June, 2026

REVIEW OF THE FUNCTIONAL CHARACTERISTICS OF A VIBRATION DYNAMIC ABSORBER

Monica BĂLCĂU, Aurora Felicia CRISTEA, Monica SAS

Abstract: *This review paper addresses a more complex engineering problem, namely, the attenuation of torsional vibrations in engine shafts in vehicles with linear or V-shafts, using dynamic absorbers. Although the theoretical framework of the specialized literature is comprehensive, the studies lack an in-depth critical analysis regarding the practical applicability and implementation of such a dynamic absorber. Designing a damper simultaneously with the overall engine structure is fundamentally different from adapting it to an isolated component. In the paper, the authors try to clearly define the operational criteria for choosing any of the strategies, depending on the specific configuration of the engine, respectively, its shaft.*

Key words: *dynamic absorber, reduced masses, vibration, angular frequency.*

1. INTRODUCTION

The introductory section notes that the specialized literature in this specific field remains limited. As established in the literature [1–8], engine configurations with a lower cylinder count exhibit increased vibration levels. Furthermore, these dynamic responses are directly influenced by operational parameters, environmental conditions, and structural infrastructure. Instead, existing publications provide more detailed and complex references for pendulum absorbers [5], which serve a distinct functional purpose compared to the dynamic vibration absorbers (DVAs) investigated in this comparative study. Dynamic absorbers are a critical solution for mitigating vibrations in vehicle engines and across various engineering fields, including civil, mechanical, aeronautic, and naval engineering [9]. In any rotating machinery, the occurrence and amplification of torsional vibrations [7] beyond permissible limits compromise engine functionality. These vibrations typically arise within the shaft assembly when the acting torsional moments exhibit large-amplitude periodic variations over short time intervals.

This paper provides a theoretical review and a comparative analysis of two studies focusing on the same functional category of dynamic absorbers. The comparison evaluates different approaches to mathematical modeling and operational simulation. To facilitate this comparative framework, the analysis is divided into two distinct configurations: Variant 1 and Variant 2. Variant 1 employs a linear dynamic absorber attached to a rectilinear elastic shaft of negligible mass, which is equipped with reduced circular masses and a flywheel [3], [7]. Conversely, Variant 2 evaluates the equivalent of a non-linear damper integrated into a V-type engine with cylinders arranged in two banks [8]. Consequently, Variant 1 investigates a dynamic absorber attached to a linear four-mass system with an equivalent mass distribution, detailing its mathematical model, dynamic equations of motion, and simulations of the resulting harmonic responses [8]. Meanwhile, Variant 2 focuses on the equivalent modeling of an absorber within a V-engine configuration,

Received: 20.04.26; **Similarities**: 12.05.26: **Reviewed**:18.05. /19.05.26: **Accepted** 09.06.26.

outlining the system equations and their respective analytical or numerical solutions.

2. DYNAMIC PERFORMANCE AND SPECIFICATIONS OF VARIANTS

Variant 1: Detailed Approach

The two configurations, designated as Variant 1 and Variant 2, are evaluated within a comparative framework to analyze the operational advantages and disadvantages of integrating each system into the vehicle engine assembly.

In Variant 1, an internal combustion engine is analyzed under the effects of fluctuating torque acting upon the crankshaft. These torsional variations are driven by inertial forces proportional to the masses that undergo both reciprocating (translational) and rotational motion within the engine's crank-slider mechanisms. These dynamic events are periodic and correspond directly to the specific phases of the thermodynamic cycle occurring inside the engine cylinders [3].

Variant 2: Detailed Approach

An optimized approach to crankshaft dimensioning allows the shaft itself to function as an inherent dynamic damper, thereby eliminating the need for supplementary components within the system. This design considers an elastic lumped-parameter model consisting of six reciprocating and rotating assemblies (comprising the pistons, connecting rods, and related components) interconnected by elastic elements of known torsional stiffness. In this context, these moving assemblies encompass the pistons, pins, and all associated reciprocating and rotating components of the crank mechanism.

2.1 Modeling and System Description

In Variant 1, an internal combustion engine is analyzed under the effects of fluctuating torque acting upon the crankshaft. These torsional variations are driven by inertial forces proportional to the masses undergoing both reciprocating and rotating motions within the engine's crank mechanisms. These dynamic events are periodic and correspond directly to the specific phases of the thermodynamic cycle occurring inside the engine cylinders [3].

An optimized approach to crankshaft dimensioning allows the shaft itself to function as an inherent dynamic damper, thereby eliminating the need for supplementary components within the system. This design considers an elastic lumped-parameter model consisting of six moving assemblies interconnected by elastic elements of known torsional stiffness. In this context, these moving assemblies encompass the pistons, pins, connecting rods, and all associated rotating components of the crankshaft.

Consequently, Variant 1 investigates a dynamic absorber attached to a linear four-mass system with an equivalent mass distribution, detailing its mathematical model, dynamic equations of motion, and simulations of the resulting harmonic responses [8].

2.1.1. Variant 1: Modeling Description

The study considers a discrete mechanical system composed of four reduced lumped masses, denoted by m_1, m_2, m_3 and m_4, according to the layout in Figure 1. These inertial elements are interconnected by the equivalent reduced sections of the crankshaft. The technical parameters of the masses and their equivalent elastic constants are denoted by u_{12}, u_{23}, u_{34} and u_{45}. Within this structural arrangement, the reduced masses and the main engine flywheel are mounted on the linear shaft. The constructive and geometric dimensions of the dynamic damper are defined by lengths l_1 and l_2, and the mass M, where the absorber mass M is attached to the last reduced mass m_4 (Figure 1). To evaluate the dynamic response, the harmonic of order *x* acting on the mechanical system is applied to the reduced masses m_1, m_2, and m_3 in the form of a time-dependent excitation force:
$P_x\cos(\Omega_x t-\varphi)$. In this mathematical relationship, P_x represents the excitation amplitude, Ω_x is the angular frequency, and φ is the phase angle. Furthermore, the parameter r defines the radius of the reduction circle from the motor shaft to the reduced mass, which corresponds directly to half of the physical piston stroke (Figure 1).

Table 1

Dimensional and technical parameters of the dynamic absorber system of Figure 1.

Parameter Category	Symbol	Value and Unit
Mass components		
First reduced mass	m_1	2661.19 g
Second reduced mass	m_2	2655.46 g
Third reduced mass	m_3	2658.40 g
Fourth reduced mass	m_4	5600 g
Absorber mass	M	150 g
Constructive dimensions		
First constructive dimension	l_1	40 mm
Second constructive dimension	l_2	10 mm
Reduction circle radius	r	40.7 mm
Dynamic & Elastic parameters		
Torsional elasticity constants	$u_{12} = u_{23} = u_{34}$	495204.67 N/mm
Fundamental angular frequency	ω_0	177.93 rad/s
Excitation force amplitude	P_x	10705 N
Harmonic order range	x	0.5 ÷ 6

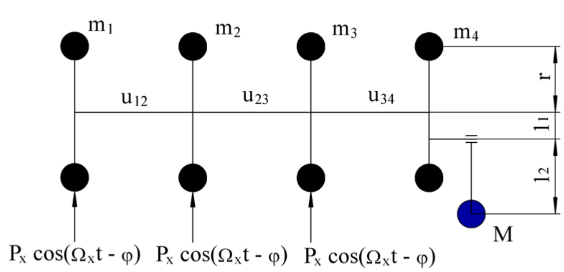

Fig. 1. Model of the dynamic absorber [3].

To facilitate the resolution of the problems that arise with this absorber, the system will be simplified in the sense of developing an equivalent system (Fig. 2) whose solutions can be more easily determined. Thus, the dynamic absorber equipment is replaced by a mechanical system consisting of a reduced mass called m_4 and a reduced shaft section having the elastic constant u_{34} (the constant u_{34}, this imposes on the system the condition of being dynamically equivalent to the dynamic absorber). In addition, the elasticity constants noted (u_{ij}) i = 1-4, j = 2-5 are close to those of the engine and are consistent with the values given in specialized books [7]. Next, the paper presents the calculated reduced masses of the absorber and initial dimensions (Table 1).

The internal combustion engine has a crankshaft driven by motor torques. The torques vary greatly during the cycle of the thermal process that takes place in the engine cylinders. In an inline engine, the crankpins are distributed along the length of the shaft in a simple and linear geometric manner.

In Table 1 and Figure 1 the notations are represented according to Table 2.

Table 2

Nomenclature and parameter descriptions for the dynamic absorber system**.**

Notation	Parameter Description	Measurement Unit
m_i	Reduced masses	[kg]
M	Absorber mass	[kg]
$P_x\cos(\Omega_x t-\varphi)$	Excitation force	[N]
l_i	Characteristic dimensions (l_1, l_2) and the mass M position	[mm]
ω_0	Angular velocity	[rad/s]
u_{ij} (i = 1 to 4)	Elasticity constants	[N/mm]

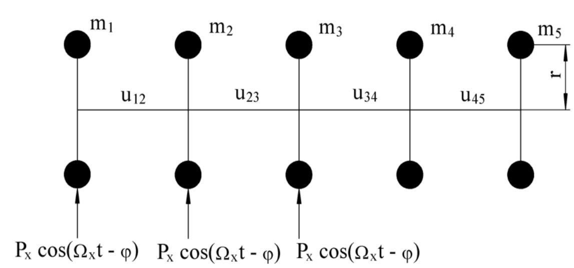

Fig. 2. Equivalent mechanical systems with reduces mass [3].

The mass moments of inertia of the rotating and reciprocating parts (pistons, connecting rods) attached to each crankpin are significantly larger than the axial mechanical moment of inertia of the shaft section between them. The variation of these torques is due to the inertia forces corresponding to the masses of the moving parts of the crankshaft, and to their translational and planar movements.

The variation of these torques is due to the inertia forces corresponding to the masses of the moving parts of the crankshaft, and to their translational and planar movements. To facilitate the analysis of these torsional vibrations in such a complex elastic system, the real system must be transformed into an equivalent dynamic system. This equivalent dynamic system consists of a rectilinear elastic shaft of negligible mass, loaded with reduced circular masses [3], where the elastic constants of the crankshaft elements depend on these four reduced masses. It is also important to choose the mass moments of inertia of the reduced masses so that the kinetic and potential energies of the real, vibrating system (formed by the crankshaft, its attached parts, and the related moving parts) are equal to those of the equivalent reduced system. System (1) represents the mechanical model shown in Figure 2 and is presented in matrix form [3] as follows:

$$[M]\{\ddot{a}\}+[U]\{a\}=\{P(t)\} \quad (1)$$

where:
[M] is the diagonal mass matrix:

$$[M] = \mathrm{diag}(m_1, m_2, m_3, m_4, 0) \quad (2)$$

[U] is the torsional stiffness matrix:

$$\begin{bmatrix} u_{12} & -u_{12} & 0 & 0 & 0 \\ -u_{12} & u_{12}+u_{23} & -u_{23} & 0 & 0 \\ 0 & -u_{23} & u_{23}+u_{34} & -u_{34} & 0 \\ 0 & 0 & -u_{34} & u_{34}+u_{45} & -u_{45} \\ 0 & 0 & 0 & -u_{45} & u_{45} \end{bmatrix} \quad (3)$$

The elongations of the torsional vibrations produced by the five reduced masses of the system will be noted according to the amplitudes A_i of the same torsional vibrations [3]:

$$a_i = A_i \cdot \cos(\Omega_x \cdot t - \varphi),\ i = 1 \div 5 \quad (4)$$

where:
A_i – system amplitudes [mm]
Δ – determinant of the system
Ω_x – angular frequency [1/s].

Substituting equations (4) and their second-order derivatives into the system of differential equations, and simplifying by the trigonometric term $\cos(\Omega_x \cdot t - \varphi)$, yields the system of algebraic equations (5).

$$\begin{aligned}
&\left(\Omega_x^2 - \frac{u_{12}}{m_1}\right)A_1 + \frac{u_{12}}{m_1}A_2 = -\frac{P_x}{m_1} \\
&\frac{u_{12}}{m_2}A_1 + \left(\Omega_x^2 - \frac{u_{12}}{m_2} - \frac{u_{23}}{m_2}\right)A_2 + \frac{u_{23}}{m_2}A_3 = -\frac{P_x}{m_2} \\
&\frac{u_{23}}{m_3}A_2 + \left(\Omega_x^2 - \frac{u_{23}}{m_3} - \frac{u_{34}}{m_3}\right)A_3 + \frac{u_{34}}{m_3}A_4 = -\frac{P_x}{m_3} \\
&\frac{u_{34}}{m_4}A_3 + \left(\Omega_x^2 - \frac{u_{34}}{m_4} - \frac{u_{45}}{m_4}\right)A_4 + \frac{u_{45}}{m_4}A_5 = 0 \\
&\frac{u_{45}}{m_5}A_4 + \left(\Omega_x^2 - \frac{u_{45}}{m_5}\right)A_5 = 0
\end{aligned} \quad (5)$$

The matrix form of the system is:

$$\begin{bmatrix} \Omega_x^2 - \frac{u_{12}}{m_1} & \frac{u_{12}}{m_1} & 0 & 0 & 0 \\ \frac{u_{12}}{m_2} & \Omega_x^2 - \frac{u_{12}}{m_2} - \frac{u_{23}}{m_2} & \frac{u_{23}}{m_2} & 0 & 0 \\ 0 & \frac{u_{23}}{m_3} & \Omega_x^2 - \frac{u_{23}}{m_3} & \frac{u_{34}}{m_3} & 0 \\ 0 & 0 & \frac{u_{34}}{m_4} & \Omega_x^2 - \frac{u_{34}}{m_4} - \frac{u_{45}}{m_4} & \frac{u_{45}}{m_4} \\ 0 & 0 & 0 & \frac{u_{45}}{m_5} & \Omega_x^2 - \frac{u_{45}}{m_5} \end{bmatrix} \cdot \begin{Bmatrix} A_1 \\ A_2 \\ A_3 \\ A_4 \\ A_5 \end{Bmatrix} = \begin{Bmatrix} -\frac{P_x}{m_1} \\ -\frac{P_x}{m_2} \\ -\frac{P_x}{m_3} \\ 0 \\ 0 \end{Bmatrix} \quad (6)$$

The harmonic angular frequency (Ω) of order x has the expression:

$$\Omega_x = x\omega_0 \quad (7)$$

The order of the harmonic (x) represents the number of oscillations that the harmonic executes. Relation (8) shows the determinant of system (1).

$$\Delta = \begin{vmatrix} \Omega_x^2 - \frac{u_{12}}{m_1} & \frac{u_{12}}{m_1} & 0 & 0 & 0 \\ \frac{u_{12}}{m_2} & \Omega_x^2 - \frac{u_{12}}{m_2} - \frac{u_{23}}{m_2} & \frac{u_{23}}{m_2} & 0 & 0 \\ 0 & \frac{u_{23}}{m_3} & \Omega_x^2 - \frac{u_{23}}{m_3} - \frac{u_{34}}{m_3} & \frac{u_{34}}{m_3} & 0 \\ 0 & 0 & \frac{u_{34}}{m_4} & \Omega_x^2 - \frac{u_{34}}{m_4} - \frac{u_{45}}{m_4} & \frac{u_{45}}{m_4} \\ 0 & 0 & 0 & \frac{u_{45}}{m_5} & \Omega_x^2 - \frac{u_{45}}{m_5} \end{vmatrix} \quad (8)$$

Using Cramer's rule, we obtain the amplitudes of the noted A_i system. For $\Delta = 0$, the natural frequencies of the system are reached. The reduced masses m_i ($i = 1$ to 4) have the vibration amplitudes given by the expressions according to reference [3]. From these expressions, after replacing the relations of the corresponding determinants, it follows that the amplitudes are:

$$A_1 \neq 0 \quad A_2 \neq 0 \quad A_3 \neq 0 \quad A_4 = 0 \tag{9}$$

The amplitudes A_1, A_2, A_3 and A_4 correspond to the vibrations of the reduced masses m_1, m_2, m_3 and m_4, derived by applying the mass and length reduction method to the crankshaft. Meanwhile, the amplitude A_5 represents the torsional vibrations of the fictitious reduced mass m_5. This mass is integrated into the reduced crankshaft model via the elasticity constant u_{45} to investigate the impact of the dynamic absorber on the crankshaft's vibrational behavior (the definitions of coefficients ui are detailed in reference [3]).

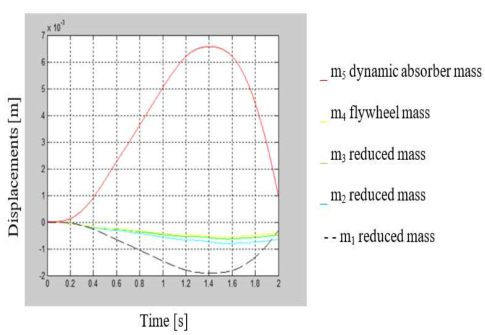

Fig. 3. Displacement graph of the moving assemblies corresponding to the reduced masses [3].

The MATLAB simulation of amplitude A_4, illustrated in Figure 3, validates the theoretical calculations, as its value (indicated in yellow) closely approaches zero. These theoretical and simulated validations will be subsequently compared with the experimental measurements performed on the engine.

From a physical standpoint, the notation u_{ij} used in the first analytical method is conceptually identical to the stiffness coefficient k_i used in the modern matrix approach (meaning $u = k$). The only mathematical distinction lies in how they are scaled: in the first approach, the stiffness coefficients are explicitly divided by the respective structural masses (u_{ij}/m_i) directly within the frequency determinant, whereas the second approach isolates the pure torsional stiffness values within a dedicated [K] matrix.

2.1.2 Variant 2: Modeling System

An optimized design of the V-engine crankshaft can enable it to function directly as a dynamic damper, thereby eliminating the need for additional components in the assembly. An elastic system, shown in Figure 4, is considered, consisting of six moving assemblies (comprising the pistons, connecting rods, and associated components) interconnected by elastic elements with known torsional stiffnesses constants and mechanical moments of inertia (J_1, J_2, $J_{1'}$, $J_{2'}$, J_3, and J_4). These moving assemblies undergo rotational motion. An excitation torque acts directly upon the final moving assembly, which has a moment of inertia denoted as J_4. The objective is to determine the operational conditions under which, under the action of this excitation torque, the vibrations of the final moving assembly are minimized. The number of degrees of freedom for this mechanical system is six ($\varphi_1, \varphi_2, \varphi_1', \varphi_2', \varphi_3, \varphi_4$).

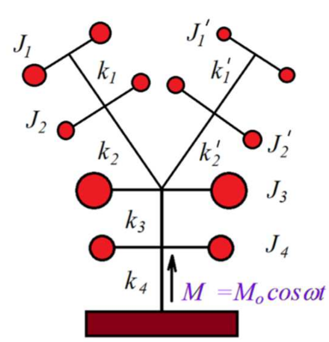

Fig. 4. Elastic system [8].

The equations of motion for the system presented in reference [8] and used data of Table 4 are expressed in matrix form as follows:

$$[J]\{\ddot{\varphi}\}+[K]\{\varphi\} = \{F(t)\} \qquad (10)$$

where:
[J] is the diagonal matrix of the moments of inertia:
$[J] = \mathrm{diag}(J_1, J_2, J_1', J_2', J_3, J_4)$

$$[J] = \begin{bmatrix} J_1 & 0 & 0 & 0 & 0 & 0 \\ 0 & J_2 & 0 & 0 & 0 & 0 \\ 0 & 0 & J_1' & 0 & 0 & 0 \\ 0 & 0 & 0 & J_2' & 0 & 0 \\ 0 & 0 & 0 & 0 & J_3 & 0 \\ 0 & 0 & 0 & 0 & 0 & J_4 \end{bmatrix}$$

[K] is the torsional stiffness matrix of the crankshaft elements:

$$[K] = \begin{bmatrix} k_1 & -k_1 & 0 & 0 & 0 & 0 \\ -k_1 & k_1+k_2 & 0 & 0 & -k_2 & 0 \\ 0 & 0 & k_1' & -k_1' & 0 & 0 \\ 0 & 0 & -k_1' & k_1'+k_2' & -k_2' & 0 \\ 0 & -k_2 & 0 & -k_2' & k_2+k_2'+k_3 & -k_3 \\ 0 & 0 & 0 & 0 & -k_3 & k_3+k_4 \end{bmatrix};$$

$\{\ddot{\varphi}\}$ and $\{\varphi\}$ are the angular acceleration and angular displacement vectors, respectively:

$$\{\ddot{\varphi}\} = \{\ddot{\varphi}_1 \;\; \ddot{\varphi}_2 \;\; \ddot{\varphi}_3 \;\; \ddot{\varphi}_4\;\}^T$$
$$\{\varphi\} = \{\varphi_1 \;\; \varphi_2 \;\; \dot{\varphi}_1 \;\; \dot{\varphi}_2 \;\; \varphi_3 \;\; \varphi_4\;\}^T$$

$\{F(t)\}$ is the external excitation torque vector acting on the system:
$\{F(t)\} = \{0\;\;0\;\;0\;\;0\;\;0\;\;M_0\cdot\cos(\omega t)\}^T$
$\{M\}$ – system mass;
[C] and [K] – the system damping and stiffness matrices, respectively;
ω – the system angular frequency.
The polynomial characteristic equation defined by the determinant of the dynamic matrix:

$$P(\omega) = \det(\,[K] - \omega^2 \cdot [M]\,) = 0 \qquad (11)$$

leads to the determination of the system's natural frequencies (eigenvalues).

Assuming a harmonic solution and requiring it to satisfy the system of differential equations yields:

$$\left(\begin{bmatrix} k_1 & -k_1 & 0 & 0 & 0 & 0 \\ -k_1 & k_1+k_2 & 0 & 0 & -k_2 & 0 \\ 0 & 0 & k_1' & -k_1' & 0 & 0 \\ 0 & 0 & -k_1' & k_1'+k_2' & -k_2' & 0 \\ 0 & -k_2 & 0 & -k_2' & k_2+k_2'+k_3 & -k_3 \\ 0 & 0 & 0 & 0 & -k_3 & k_3+k_4 \end{bmatrix} - \omega^2 \begin{bmatrix} J_1 & 0 & 0 & 0 & 0 & 0 \\ 0 & J_2 & 0 & 0 & 0 & 0 \\ 0 & 0 & J_1' & 0 & 0 & 0 \\ 0 & 0 & 0 & J_2' & 0 & 0 \\ 0 & 0 & 0 & 0 & J_3 & 0 \\ 0 & 0 & 0 & 0 & 0 & J_4 \end{bmatrix}\right) \cdot \begin{Bmatrix} a_1 \\ a_2 \\ a_1' \\ a_2' \\ a_3 \\ a_4 \end{Bmatrix} = \begin{Bmatrix} 0 \\ 0 \\ 0 \\ 0 \\ 0 \\ M_0 \end{Bmatrix} \qquad (12)$$

Where the amplitudes of the harmonic oscillations are contained in the vector:

$$\{A\} = [a_1\; a_2\; a_1'\; a_2'\; a_3\; a_4]^T \qquad (13)$$

To find the required conditions for $a_4 = 0$, the determinant of the system [9] becomes:

$$[C] = \begin{bmatrix} k_1-\omega^2 J_1 & -k_1 & 0 & 0 & 0 & 0 \\ -k_1 & k_1+k_2-\omega^2 J_2 & 0 & 0 & -k_2 & 0 \\ 0 & 0 & k_1'-\omega^2 J_1' & -k_1' & 0 & 0 \\ 0 & 0 & -k_1' & k_1'+k_2' & -k_2' & 0 \\ 0 & -k_2 & 0 & -k_2' & k_2+k_2'+k_3-\omega^2 J_3 & -k_3 \\ 0 & 0 & 0 & 0 & -k_3 & k_3+k_4-\omega^2 J_4 \end{bmatrix};$$

$$[C_{11}] = \begin{bmatrix} k_1-\omega^2 J_1 & -k_1 & 0 & 0 & 0 \\ -k_1 & k_1+k_2-\omega^2 J_2 & 0 & -k_2 & 0 \\ 0 & 0 & k_1'-\omega^2 J_1' & -k_1' & 0 \\ 0 & 0 & -k_1' & k_1'+k_2'-\omega^2 J_2' & -k_2 \\ 0 & 0 & 0 & -k_2' & k_2+k_2'+k_3-\omega^2 J_3 \end{bmatrix} \qquad (14)$$

The operational values considered in this study are listed in Table 3:

Table 3

System amplitudes [8].

Frequency	**A_1**	**A_2**	**A_3**	**A_4**	**A_5**	**A_6**
[Hz]	198.5	671.12	729.7	1094	1248	2172

Table 4

System parameters.

Parameters	
$J_1 = 1.0$ kgm^2	$k_1 = k_{10} = 1,\ 000,\ 000$ Nm/rad
$J_2 = 3.0$ kgm^2	$k_2 = k_{20} = 3,\ 000,\ 000$ Nm/rad
$J_{10} = J_1' = 1.0$ kgm^2	$k_3 = 2,\ 000,\ 000$ Nm/rad
$J_{20} = J_2' = 6.0$ kgm^2	$k_4 = 1,\ 000,\ 000$ Nm/rad
$J_3 = 2.0$ kgm^2	
$J_4 = 6.0$ kgm^2	
The excitation torque: M = 10, 1000 Nm.	

Figure 5 presents the vibration amplitudes of all six moving assemblies.

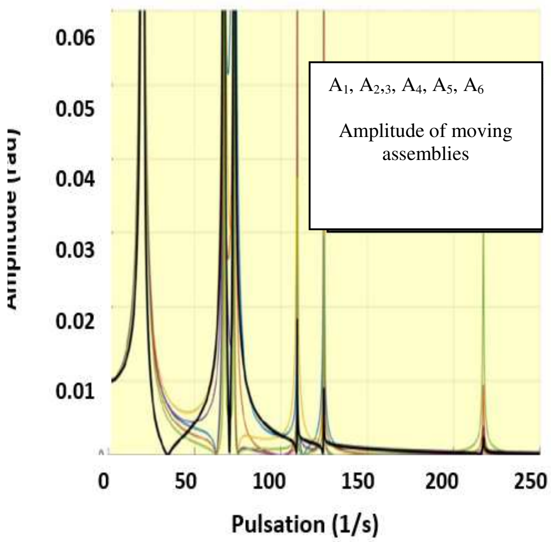

Fig. 5. Vibration amplitudes of the moving components (the black curve represents the response of the 6-cylinder assembly) [8].

Figure 6 and Table 3 present the angular frequency intervals that ensure a zero-amplitude state for the sixth moving assembly. For each moment of inertia value of the second cylinder mechanism, five distinct frequencies are identified where total vibration absorption occurs for this specific assembly.

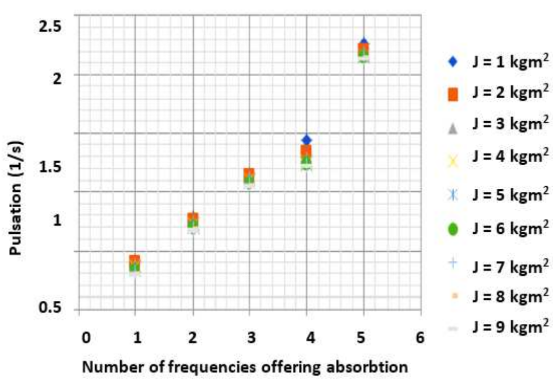

Fig. 6. Angular frequency intervals ensuring a zero-amplitude state for the sixth moving assembly at distinct moments of inertia of the second assembly [8].

3. DISCUSSIONS ON SYSTEMATIC EVALUATION AND ENGINEERING COMPARISON

To provide clear guidance for automotive powertrain design and address the gaps in existing literature, Table 5 benchmarks Variant 1 and Variant 2 against industry-standard alternatives, specifically Tuned Mass Dampers (TMD) and Centrifugal Pendulum Vibration Absorbers (CPVA).

Table 5

Comparative analysis of structural parameters and damping strategies.

Damping Strategy	Applicable Layout	DOF	Main Engineering Advantage	Critical Operational Limitation
Variant 1 (Linear)	Standard in-line	5	High attenuation at a single resonant frequency.	Ineffective under transient speeds or variable loads. Note. The axial moment of inertia of the shaft sections is neglected by adopting the lumped mass model, due to the inline geometry and the significantly higher weight of the attached masses (pistons, connecting rods).
Variant 2 (Nonlinear)	V-type engine layout	6	Leverages inherent crankshaft geometry; zero mass.	Complex manufacturing tolerances; limited bandwidth.
Tuned Mass (TMD)	Universal automotive	Multi	Proven, robust external solution for broad damping.	Increases total powertrain mass and package space.
Centrifugal (CPVA)	Modern high-torque	Non-lin	Automatically tunes to multiple harmonic orders.	High structural complexity and manufacturing costs.

A comparative analysis of these two approaches reveals that the shift in notation is not merely a symbolic preference among different authors, but a technical necessity dictated by the specific engine architecture.

While the first theoretical formulation (using the (u_{ij}/m_i) notation) is tailored to standard in-line crankshafts where each node corresponds to a single cylinder with symmetrical dynamics, the second approach addresses V-type configurations.

In a V-engine, two distinct slider-crank mechanisms operate on a single crankpin, generating complex torsional excitation components and geometric variations in the moments of inertia. Consequently, transitioning to the modern [K] matrix formalism with individualized stiffnesses (k_i) becomes essential; it enables proper matrix substructuring for V-configurations and accurately couples them with asymmetric excitation vectors. Nevertheless, although the discretization techniques differ in granularity due to topology, both methods converge toward identical results, determining the exact same fundamental natural frequencies of the system.

From a physical standpoint, the notation u_{ij} used in the first analytical method is conceptually identical to the stiffness coefficient k_i used in the modern matrix approach (meaning $u_{ij} = k_i/m_i$ when evaluating the normalized structural dynamics). The only mathematical distinction lies in the architectural formulation and how these scaling factors are handled within the governing differential equations of motion. In the first approach, the localized stiffness coefficients are explicitly divided by their respective structural lumped masses directly within the fundamental frequency determinant, creating a highly coupled numerical form tailored for manual or semi-analytical calculations. Conversely, the second approach utilizes advanced computational layouts to completely isolate the pure torsional stiffness values within a dedicated, independent stiffness matrix [K], while storing the inertial properties inside a separate mass matrix [M].

The systematic evaluation presented in Table 5 clearly contextualizes the operational boundaries and damping capabilities of both analyzed variants within the framework of state-of-the-art vehicular attenuation technologies. This comparative matrix serves as an engineering tool to visualize how traditional analytical assumptions perform when coupled with modern external absorbers under different engine load profiles. Based on this thorough technical evaluation and the structural trade-offs identified across the distinct in-line and V-type engine layouts, the final overarching assessments, major literature gaps, and practical engineering guidelines for powertrain manufacturing are formulated in the subsequent section.

4. CONCLUSIONS

This review paper investigated two distinct dynamic vibration attenuation strategies for internal combustion engine crankshafts. By systematically analyzing the theoretical modeling, simulated behaviors, and structural frameworks of both systems [3, 6, 8], and integrating them with the comparative metrics developed in this study, the following final engineering insights, advantages, and critical limitations are concluded:

a) Advantages and Design Insights: Analytical Viability of Variants 1 and 2

- **Variant 1 (Linear Model)**: The linear dynamic framework offers a reliable, low-complexity analytical approach to suppress torsional resonance at fixed critical nodes in standard in-line powertrains. Utilizing a dynamic absorber with lumped masses and a flywheel on a linear shaft [3], the total number of resonance frequencies decreases by exactly one unit, validated via the classical relative displacement relation (u_{ij}/m_i).
- **Variant 2 (V-type Engine)**: The modern structural equivalent framework maps the complex physical symmetry of V-type engines with cylinders in two banks [8]. It accurately captures coupled dynamic interactions through the stiffness matrix [K] with 6 degrees of freedom and moments of inertia J_1-J_4, without relying on expensive hardware.
- **Sizing Efficiency**: Both configurations validate optimized concurrent crankshaft dimensioning, proving the shaft can serve a dual structural and damping role to reduce vehicle mass and save engine compartment space.

b) Numerical Evaluation Methodology and Integration of Industry Systems (Table 5)

- **MATLAB Approach**: To bridge gaps in the evaluated literature [3, 8], a comparative numerical methodology was applied. Matrix computation algorithms extracted eigenvalues and eigenvectors for the 6-DOF system. Parallel execution for both variants confirmed the mathematical identity of the natural frequency spectrum obtained through classical and modern methods.
- **Damping Systems Evaluation**: This evaluation was extended in **Table 5** to standard crankshaft behavior against industry solutions [6]: Tuned Mass Dampers (**TMD**) and Centrifugal Pendulum Vibration Absorbers (**CPVA**). Numerical trends show that the TMD isolates resonances at fixed engine speeds, while the CPVA dynamically adapts its frequency response, tracking critical orders across the entire V-engine operating range.

c) Disadvantages, Critical Limitations, and Future Research Guidelines

- **Lack of Practical Design Rules**: The frameworks examined in the evaluated literature [3, 8] remain predominantly descriptive and theoretical. They fail to distill actionable, parametric design boundaries or concrete engineering rules that can be directly implemented into the industrial manufacturing workflow of crankshafts.
- **Need for Experimental Validation**: Although the MATLAB simulations provide a solid preliminary graphical trend for the theoretical validation of the models, the evaluated studies [3, 8] often omit strict numerical convergence metrics or structured error analyses. The critical direction for future research consists of directly correlating the developed numerical comparison with real physical experimental data obtained via direct telemetry on an engine test bench.

5. REFERENCES

[1] W. G. Ata, A. M. Salem, *Experimental Characterization and Nonparametric Modeling of Armored Vehicle Hydraulic Shock Absorber Under Periodic Excitations*, Journal of Vibration Engineering & Technologies (2025) 13:311 , https://doi.org/10.1007/s42417-025-01830-9.

[2] M. C. Bălcău, A. F. Cristea, *Experimental studies regarding the use of dynamic absorbers in the assembly of engines of vehicles*, 4th International Conference on Control, Artificial Intelligence, Robotics, and Optimization ICCAIRO 2023 11-13 April 2023 Ierapetra, Greece, http://www.iccairo.com, accessed 12.02.2024, 979-8-3503-0091-8/23/$31.00 ©2023 IEEE, doi: 10.1109/ICCAIRO58903.2023.00012, 2023, pp.19-25.

[3] Bălcău M., Cristea A. F., "*Contributions on the use of dynamic absorbers in a vehicle engine*", WSEAS TRANSACTIONS on APPLIED and THEORETICAL MECHANICS, Engineering World, 2024, DOI 10.37394/232025.2024.6.18, E-ISSN 2692-5079, vol.6, pp 170-179.

[4] F. Carollo, G. V. Mariotti, S. Golfo, A. Pappalardo, Dynamic Tests of Formula SAE Car Bodies, WSEAS Transactions on Systems, vol. 21, 2022, pp. 104-114.

[5] G. A. Haddow, S. W. Shaw, *"Centrifugal pendulum vibration absorbers: an experimental and theoretical investigation",* Nonlinear Dynamics 34: Kluwer Academic Publishers. Printed in the Netherlands, 2004, pp. 293–307.

[6] R. Nair, K.I. Ramachandran, *Design and optimization of automotive energy absorber structure with functionally graded material*, Volume 5, Issue 11, Part 3, 2018, Pages 25640-25648, https://doi.org/10.1016/j.matpr.2018.11.005.

[7] A. Ripianu, I. Crăciun, "*The dynamic and strength calculus of straight and crank shafts"*, Transilvania Press Publishing House Cluj, 1999.

[8] M. L. Scutaru, M. Marin, S. Vlase, *Dynamic Absorption of Vibration in a Multi Degree of Freedom Elastic System*, Mathematics, **2022**, *10*(21), 4045;

https://doi.org/10.3390/math10214045, https://www.mdpi.com/2227-7390/10/21/4045.

[9] Q. Sun, Y. Wen, Z. Ji, Y. Zou, *Modeling and simulation of composite vibration absorber for urban rail vehicle body*, Zhendong yu Chongji/Journal of Vibration and Shock 39(21):203-210, DOI:10.13465/j.cnki.jvs.2020.21.027, November 2020. https://www.researchgate.net/publication/357093261

Review privind caracteristicile funcționale ale unor absorbitoare dinamice de vibrații

Rezumat: Această lucrare de sinteză abordează o problemă inginerească complexă: atenuarea vibrațiilor torsionale din arborii motori ai vehiculelor cu cilindri în linie sau în V, utilizând absorbitorul dinamic. Deși literatura de specialitate oferă un cadru teoretic cuprinzător, studiilor existente le lipsește o analiză critică aprofundată privind aplicabilitatea practică și implementarea unui astfel de dispozitiv. Proiectarea unui amortizor integrat în structura globală a motorului diferă fundamental de adaptarea acestuia pe o componentă izolată. Astfel, autorii definesc clar criteriile operaționale pentru alegerea fiecărei strategii, în funcție de configurația specifică a motorului și a arborelui acestuia.

BĂLCĂU Monica, Lector PhD Eng., Technical University of Cluj - Napoca, Faculty of Automotive, Mecatronics and Mechanical Engineering, Blvd. Muncii no. 103-105, tel: 0741.192.423, Cluj-Napoca, Romania, e-mail: monica.balcau@auto.utcluj.ro.

CRISTEA Aurora Felicia, Assoc. prof. PhD Eng., Technical University of Cluj - Napoca, Faculty of Industrial Engineering, Robotics and Production Management, Blvd. Muncii no. 103-105, tel: 0721.917.061, Cluj-Napoca, Romania, e-mail: felicia.cristea@mep.utcluj.ro.

BOCA-SAS Monica, Lector PhD Eng., Technical University of Cluj - Napoca, Faculty of Materials and Environmental Engineering, Blvd. Muncii no. 103-105, Cluj-Napoca, Romania, e-mail: Monica.Sas.Boca@ipm.utcluj.ro.